Viser Technology Pte. Ltd.
Research and Application of Materials Science
DOI: 10.33142/rams.v3i2.6731

Research Article Open Access

An Effective Way to Prepare Submicron MoO_2 Anodes for High- Stability Lithium-Ion Batteries

Xiu-Lan LI, Jian LIN, Cui-Yan TONG*, Hai-Zhu SUN*

National & Local United Engineering Laboratory for Power Battery, College of Chemistry, Northeast Normal University, Changchun, China

***Corresponding Author:** *Hai-Zhu SUN and Cui-Yan TONG, 5268 Renmin Street, Changchun, 130024, P. R. China; sunhz335@nenu.edu.cn;tongcy959@nenu.edu.cn*

Abstract:
Herein, MoO_2-based submicrons (named MoO_2@C) are synthesized through an effective one-step hydrothermal process. The prepared MoO_2 submicrons wrapped in carbonouse layer are uniformly produced and can be applied to the anodes in lithium-ion batteries (LIBs). The novel MoO_2@C electrodes demonstrate attractive lithium storage ability. Moreover, compared with the commercial pure MoO_2, the MoO_2@C delivers a superior electrochemical capacity (e.g, 760.83 mAh g^{-1} capacity in long-life test at high rate of 1 A g^{-1}) with outstanding capacity retention ratio and stability as well as rate capability. The superior lithium storage capabilities result from plenty of the Li^+ sites and adequate electrolyte infiltration effect, which allows the fast transport of electrons and ions, and well-dispersed MoO_2 submicrons in carbon-based layers that effectively prevents aggregation of nano size particles.
Keywords: *submicrons; MoO_2; Carbon coating; Lithium-ion battery*

1 Introduction

Increasing of environmental and energy problems has triggered strong research interests in the use of sustainable and renewable energy storage devices [1-4]. As a new emerging Mo-based material applying in LIBs, potential MoO_2 equips with the intrinsic metallic nature (bulk electrical conductivity up to 1.1×10^6 Ω^{-1} m^{-1} at 300 K) and the low electrical resistivity with one-dimensional (1D) tunnel structure, which can significantly facilitate Li^+ and electron transport kinetics [5-7]. Moreover, MoO_2 with the high density of 6.5 g cm^{-3}, which is about 3.25 times compared with commercial graphite (2 g cm^{-3}), makes it possible to obtain 7.3 times capacity of graphite under similar volume condition [8-11]. Therefore, MoO_2 anodes have been given great interests to the field of lithium-ion batteries (LIBs). However, the three major bottlenecks limit its practical full cell application. (i) The pulverization results in poor cyclic capacity and capacity faded phenomenon because of the fully conversion reaction possesses [12-13]. (ii) The unsatisfying rate performance results from relatively low conductivity [14-15] (iii) The sluggish kinetics limit lithium-ion transportation in bulk MoO_2. Therefore, it is great challenge to prepare MoO_2 based electrode materials.

Preparing the nano-sized MoO_2@C is an effective solution to the bottlenecks. Usually, MoO_2 is prepared by the reduction of MoO_3[16-18]. In the synthesis process, MoO_3 is treated under a hydrogen atmosphere at high temperature, followed by the formation of large particles. For example, Song et al. adopted the ultrasonic spray pyrolysis to make spherical molybdenum dioxide materials. The precursor solution was prepared using aqueous ammonium molybdate and sucrose as the reducing agent and carbon source, and the ultrasonic spray pyrolysis was carried out at 550-650℃ under 5% H_2 / Ar atmosphere. Spheres with diameters of 2-6 μm were obtained[19]. Zhang et al. used ammonium hepta-molybdate tetrahydrate as a precursor and polyvinylpyrrolidone as a modifier to first prepare molybdenum trioxide nanoparticles by hydrothermal synthesis, and then obtained molybdenum dioxide nanoparticle by high temperature reduction at 420 ℃ under argon-hydrogen atmosphere, with nanoparticle size around 300 nm[20].

In this work, a nano-spherical MoO_2@C material with an average particle size of ～200 nm is prepared by the simple hydrothermal method without any impurities, which is a very competitive way for large scale production. Besides, for the green chemical concept, the biomass gelatin is selected as carbon source. The structure, morphology, and electrochemical properties of the MoO_2@C composite are investigated using various analytical techniques. Particularly, the MoO_2@C anode shows the better long-term stability compared with pure MoO_2. The rate-capability and capacity retention of the synthesized material are significantly improved compared with the commercial pure MoO_2 (5

Received on September 28, 2021; Accepted on December 17, 2021

times capacity enhancement at 1 A g^{-1} in the cycling test). The experimental results show that the uniform carbon distribution and nano-sized particle offer more adsorption sites to shorten the ion transport pathway resulting from the effective routine. Furthermore, the analysis tests indicate that there is no damage for the structure of MoO_2@C after working 1000 cycles. Therefore, this work may offer a novel strategy for design of nano-size particles electrode materials with high-performance for Li^+ based energy storage devices.

2 Experimental Section

2.1 Materials

Ammonium molybdate tetrahydrate ($(NH_4)_6Mo_7O_{24}\cdot 4H_2O$), gelatin and sodium hydroxide (NaOH) were purchased from Aladdin company. All chemical reagents are used without purify.

2.2 Preparation of MoO_2@C.

Typically, 0.50 g $(NH_4)_6Mo_7O_{24}\cdot 4H_2O$ was stirred for 30 min in 25 mL deionized water. Then, gelatin (0.76 g) was added and stirred for 30 min (80℃). After that, 1 mL NaOH (1 M) solution was injected into it with ultra-stir for 15 min. Finally, the uniform solution was transferred in Teflon reactor (capacity: 50 mL). After reacting at the 200℃ for 24 h, the product was washed with water and ethanol two times, respectively. The prepared black powder was transferred in tube furnace with the heating process at the 500℃.

2.3 Material characterizations

The powder X-ray diffraction using Cu Kα radiation (XRD, Smartlab 2200PC) was implemented to identify the phase of MoO_2@C. To figure out the size, morphology and the element distribution in MoO_2@C, field-emission scanning electron microscopy (SEM)and energy dispersive X-ray spectroscopy (EDX) were performed (HITACHI SU8010).

2.4 Electrochemical measurements

Blade-coating method was adopted to prepare the working electrodes. The materials weighted at the ratio of 7:2:1 (MoO_2@C / carbon black / polyvinyl difluoride) in proper amount of N-methylpyrrolidone (NMP). After stirred for one day, the slurry was rapidly bladed onto the copper foils and dried in the 80℃ condition.

The typical LIBs were assembled as followings in Ar-filled glovebox (SUniversal 2440/750). The pure lithium foil was used as counter electrode while MoO_2@C as the working electrodes, and 150 μL electrolyte (1.0 mol/L $LiPF_6$ in ethylene carbonate / dimethyl carbonate) as the electrolyte. The current density and capacity were calculated ～1 mg as the benchmark.

To value the electrochemical reaction, galvanostatic discharge/charge curves (GCD) and cyclic voltammetry (CV) were tested (LAND CT2001A). The electrochemical impedance spectra (EIS) was carried out on electrochemistry workstation (CHI750E) with a ±5 mV ac signal amplitude and a frequency ranged from 10 kHz to 0.01 Hz.

All the electrochemical tests were conducted at ～25℃.

3 Results and Discussion

Figure 1 schematically illustrates the formation of MoO_2@C submicrons. MoO_2@C was first synthesized by employing a hydrothermal process with $(NH_4)_6Mo_7O_{24}\cdot 4H_2O$ and gelatin, and then annealed to form nanostructured MoO_2@C. Nanostructured MoO_2@C will have a large surface area and more active sites, thus improving the kinetics of Li^+.

Figure 1 Schematic of the synthesis of the MoO_2@C.

The phase composition and crystal structure of MoO_2@C is further obtained by XRD. As shown in Figure 2a, the obtained composites are in good agreement with the space group p63/mmc (JCPDS: 37-1492) of pure MnO_2. The distinct diffraction peaks at 36.52°, 38.10°, 41.37°, 53.80° and 65.73° correspond to the (100), (002), (101), (102) and (110) planes, respectively. Moreover, the peak width at half width of diffraction peaks with strongly intensity suggests a small particle size and high crystallinity of MoO_2, consistent with the characteristics of pure MoO_2. Besides, the baseline of the XRD pattern increases considerably during 20-30°, which proves the occurrence of an amorphous carbon. All of these characterizations further confirm the successful preparation of the highly crystalline pure phase MoO_2@C sample.

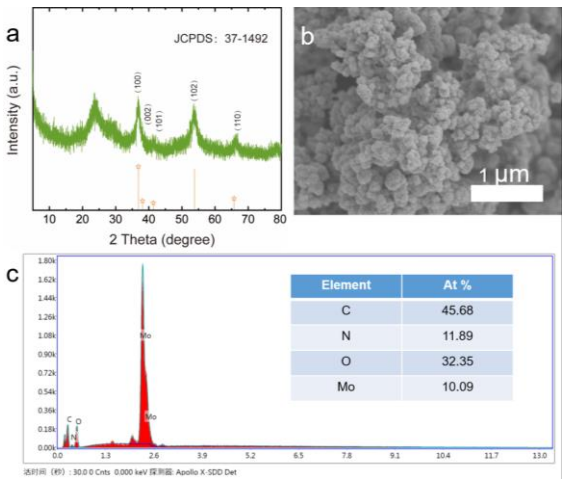

Figure 2 The characterizations of MoO_2@C (a) The XRD pattern. (b) The SEM image showing the average particle size with ～200 nm. (c) The EDX results of Mo, O, C and N

To further determine the structure, several tools were used to analyze the nanostructures and characterize the distribution of elements in the nanostructures. MoO_2@C is studied by SEM. SEM image shows the morphology and microstructure of MoO_2@C. It clearly presents uniform and smooth solid sphere with an average particle radius of about 200 nm (Figure 2b). After high temperature annealing treatment, the spheres still preserve its structure, indicating the stable structure.

Furthermore, as shown in Figure 2c, the EDX image shows the existence of Mo, O, N and C species with 10.09%, 32.35%, 11.89% and 45.68%. It is noticeable that gelatin plays a double functional role, as a reducing agent and a carbon source at the same time in the composite. On the grounds of the above results, it is confirmed the successful preparation of spherical MoO_2@C with nanoscale size.

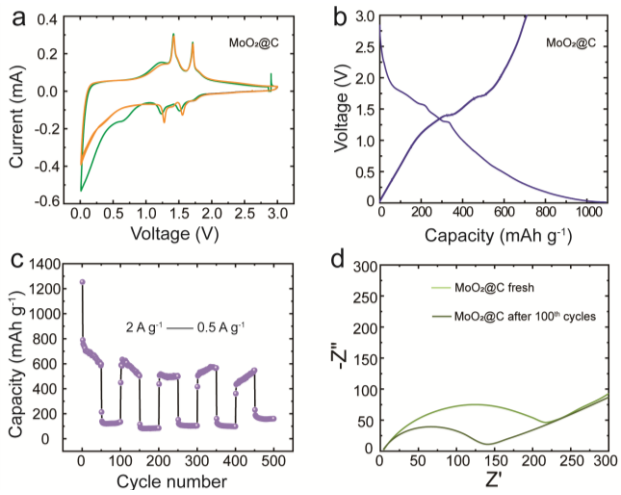

Figure 3 The electrochemical performances of MoO_2@C. (a) The first three cycles of CV curves. (b) The GCD curves. (c) The rate performances with 2 A g^{-1} charge and 0.5 A g^{-1} discharge. (d) The EIS image of MoO_2@C fresh and MoO_2@C after 100 cycles

To further explore the potential applicability of MoO_2@C as an anode material in LIBs, the typical button cells were assembled in the glove box and tested. As illustrated in Figure 3a, the CV of the MoO_2@C electrode is monitored over a voltage range in 0.01-3.0 V with a scan rate of 0.1 mV s^{-1}. In the first cycle, two cathodic of peaks are clearly observed at 1.25 V and 1.52 V. This mechanism of lithium ion insertion and de-insertion reaction is the same as that already reported in the paper[21]. The two cathodic peaks are in relation to the phase transition from monoclinic to orthoclinic of MoO_2 during Li^+ insertion. In accordance with the study of Dahn and McKinnon, the two oxidation peaks located at 1.47 V and 1.7 V are shown in the lithium extraction process[22]. The reduction peak that is located at ～0.6 V can be attributed to the formation of a solid electrolyte interphase (SEI) film between the MoO_2 submicrons and the electrolyte. The second cycle, the CV curve remains stable; meanwhile, its redox peaks are basically the same as the first cycle, located at 1.25V/1.47V and 1.52V/1.7V, respectively. This indicates that an irrecoverable reaction occurs during the initial Li^+ insertion, and then, no noticeable changes are observed in the subsequent cycles. The obtained potential shows that the material has good reversibility. At the same time, the polarization of the electrode material can be alleviated.

The GCD was valued in the potential range of 0.01-3 V, which is the area where the insertion/extraction reaction is known. Figure 3b reveals the voltage curves of the nanoscale MoO_2@C composite electrode. The first discharge and charge capacities are approximately 1363.51 mAh g^{-1} and 937.09 mAh g^{-1}, and the initial Coulombic efficiency (ICE) is 68.73%, which is mainly attributed to the irreversible lithium intercalation into the carbon. This is well coordinated with the broad peak observed in the CV curve. Other irreversible processes such as some lithium trapped in the MoO_2 lattice, the formation of SEI, and the pyrolysis of electrolyte can also affect the ICE. The reversible discharge capacity of the MoO_2@C compound is higher than its theoretical capacity, which can be attributed to the better Li^+ occupancy in the near-surface environment due to the nanoscale native particles of MoO_2[23]. Meanwhile, in the first cycle, two different discharge plateaus (0.5-1.0 V and 1.0-1.5 V) and charging plateaus (1.0-1.5 V and 1.5-2.0 V) can be observed, which is in good agreement with the oxidation and reduction peaks in the CV curves.

Besides, the MoO_2@C composition also shows a remarkably high-rate capability (Figure 3c). A high current charge is first set and cycled for 50 turns with an approximate specific capacity of ～120 mAh g-1; then a low current discharge is set and cycled for 50 turns with a specific capacity of ～510 mAh g-1, and continues to circulate 500 cycles. It is observed that the specific capacity of the electrode basically remains stable, indicating that the electrode material structure is stable.

To further understand the electrochemical reaction kinetics of MoO_2@C, EIS measurements were performed. Figure 3d shows the Nyquist plots of MoO_2@C in fresh and after 100 cycles. SEM image after cycling is shown in the inset. It is shown that each Nyquist plot consists of a depressed semicircle at high frequencies, a semicircle at medium frequencies, and a tilted line at low frequencies. They correspond to the migration resistance of lithium ions in the SEI interface layer, the charge transfer resistance, and the solid diffusion resistance of lithium ions in the active material, respectively. By comparing the two Nyquist plots, the diameter of the semicircle decreases significantly after cycling, which is attributed to electrochemical activation. It is worth noting that the tilt lines remain parallel throughout the cycling process, indicating that the solid diffusion of lithium ions is always stable. The EIS results indicate that the composite has relatively low impedance and fast Faraday reaction kinetics, consistent with its superior rate performance.

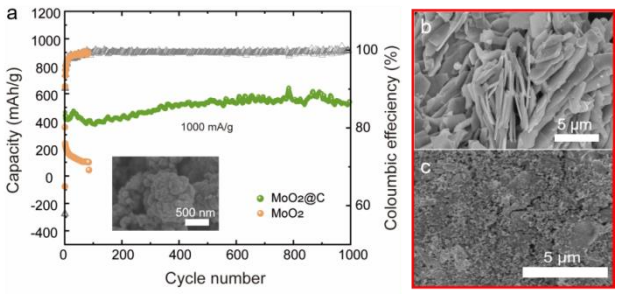

Figure 4 (a) The electrochemical cycling performances comparison of MoO_2@C and commercial MoO_2 and the inset image is the SEM image of MoO_2@C nanocomposites after cycling. (b, c) The SEM images of commercial MoO_2 before and after cycling

Remarkably, the long-term cycling stability tests at high current densities (1 A g^{-1}) show a discharge capacity of 760.83 mAh g^{-1} with capacity retention of ～69.75% (Figure 4a). During the cycles, all capacities show a tendency to increase and then smooth. This is due to the slow activation of the material makes the infiltration of the electrolyte after a period of time. As a point of comparison, the plain MoO_2 electrode display a much lower capacity of 231.00 mAh g^{-1} after the 84 loops at 1 A g^{-1} and an obvious decrease trend during electrochemical process. By comparing the SEM image of the MoO_2@C nanocomposites inside the Figure 4a, the SEM images of pure MoO_2 before and after cycling indicating that the structure of MoO_2 submicrons seriously break and collapse (Figure 4b, c). For the MoO_2@C, the structure still maintained a stable microstructure after cycling (the inset image in Figure 4a). Because the carbon coating can effectively mitigate the volume expansion of MoO_2 submicrons during the charge/discharge process and avoid the fragmentation of the electrode material.

4 Conclusion

In summary, a green and simply hydrothermal assisted method is adopted to synthesize MoO_2@C nanocomposites. As anode materials for Li-ion batteries, MoO_2@C nanocomposites demonstrate higher specific capacitance and more stable cycling ability than pure MoO_2. Besides, the MoO_2 submicrons that are embedded in amorphous carbon effectively improve the electrical conductivity and decrease the cycling resistance. Combined with lithium metal to aggregate the LIBs, the MoO_2@C anode displays a high initial discharge capacity of 760.83 mAh g^{-1} at 1 A g^{-1} and a long-time cycling stability of ～69.75% after performing 1000 cycles. All these results indicate that the MoO_2@C nanocomposites synthesized in this work have potential application in LIBs.

Author Contributions: X.L. Li and J. Lin were contributed this work equally. X.L. Li, J. Lin, and H. Z. Sun are contributors in this work. X.L. Li performed the whole experiment including samples preparation, electrode preparation, the cell assembly in a glove box and the measurement of electrochemical properties of the cycling and rate performance, the CV curves, the EIS test. J. Lin helped to characterize the morphology features such as SEM, TEM and XRD measurements and analyse the obtained results. Professor H.Z. Sun. supervised the project, wrote and revised the whole manuscript.

Conflict of Interest: No conflict of interest was reported by the authors.

Fund Project: Financial supports from the NSFC (22035001, 21574018, and 51433003), the Fundamental Research Funds for the Central Universities (2412019ZD002).

References

[1] Gu Z Y, Guo J Z, Sun Z H, et al., Air/water/temperature-stable cathode for all-climate sodium-ion batteries. Cell Reports Physical Science 2021, 2: 100665.

[2] Liang H J, Gu Z Y, Zhao X X, et al., Ether-based electrolyte chemistry towards high-voltage and long-life Na-ion full batteries. Angewandte Chemie International Edition 2021, 60: 26837.

[3] Zhao C D, Guo J Z, et al., Flexible quasi-solid-state sodium-ion full battery with ultralong cycle life, high energy density and high-rate capability. Nano Research 2022, 15: 925.

[4] Heng Y, Gu Z, et al., Research Progresses on Vanadium-based Cathode Materials for Aqueous Zinc-Ion Batteries. Acta Physico-Chimica Sinica 2021, 37: 2005013.

[5] Zhang H J, Shu J, et al., Lithiation mechanism of hierarchical porous MoO_2 nanotubes fabricated through one-step carbothermal reduction. Journal of Materials Chemistry A 2014, 2: 80-86.

[6] Y Wang, L Yu, et al., Formation of Triple-Shelled Molybdenum–Polydopamine Hollow Spheres and Their Conversion into MoO_2/Carbon Composite Hollow Spheres for Lithium-Ion Batteries. Angewandte Chemie International Edition 2016, 55: 14668-14672.

[7] Nithyadharseni P, Reddy M V, et al., Sn-based intermetallic alloy anode materials for the application of lithium ion batteries. Electrochim Acta 2015, 161: 261-268.

[8] Chen Z, Yang T, et al., Single Nozzle Electrospinning Synthesized MoO_2@C Core Shell Nanofibers with High Capacity and Long-Term Stability for Lithium-Ion Storage. Advanced Materials Interfaces 2017, 4: 1600816.

[9] Sun Y, Hu X, et al., Ultrafine MoO_2 nanoparticles embedded in a carbon matrix as a high-capacity and long-life anode for lithium-ion batteries. Journal of Materials Chemistry 2012, 22: 425-431.

[10] Yang L, Li X, Gao Q, et al., Hierarchical MoO_2/Mo_2C/C Hybrid Nanowires as High-Rate and Long-Life Anodes for Lithium-Ion Batteries. ACS Applied Materials and Interfaces 2016, 8: 19987-19993.

[11] Yang S, Feng X, et al., Fabrication of graphene-encapsulated oxide nanoparticles: towards high-performance anode materials for lithium storage. Angew. Chem. Int. Ed 2010, 49: 8408-8411.

[12] Zhang W M, Hu J S, et al., Tin-nanoparticles encapsulated in elastic hollow carbon spheres for high-performance anode material in lithium-ion batteries. Adv. Mater 2008, 20: 1160-1165.

[13] Qu Q, Gao T, et al., Strong surface-Bound Sulfur in Conductive MoO_2 Matrix for Enhancing Li-S Batterery Performance.Advanced Materials Interfaces 2015, 2(7): 150201-150206.

[14] Lu P, Xue D, et al., Hollow Nanostructured MoO_2 Electrode Materials for Supercapacitors. Materials Focus 2012, 1(2): 131-135.

[15] Palanisamy K, Kim Y, et al. Self-assembled Porous MoO_2/giaphene Microspheres towards High Performance Anodes for Lithium Ion Batteries. Journal of Power Sources 2015, 275: 351-360.

[16] Zhang R H, Hao Z H, et al., Mechanism of Non-Contact Reduction of MoO_3 to Prepare MoO_2. JOM 2022, 10: 22-24.

[17] Wang L, Zheng L X, et al., Mechanism and Kinetic Study of Reducing MoO_3 to MoO_2 with CO–15 vol % CO_2 Mixed Gases. ACS Omega 2019, 10: 1021-1030.

[18] Sun G D, Zhang G H, et al., Study on the reduction of commercial MoO3 with carbon black to prepare MoO_2 and Mo_2C nanoparticles. International Journal of Applied Ceramic Technology 2020, 10: 13473-13476.

[19] Song J H, Kang H J, et al., Electrochemical Characteristics of MoO_2 Anode Materials with Various Morphologies for LIB Applications. ECS Meeting Abstracts 2009, 2: 479.

[20] Zhang X Q, Hou Z G, et al., MoO_2 nanoparticles as high capacity intercalation anode material for long-cycle lithium ion battery. Electrochimica Acta 2016, 213: 416-422.

[21] Zhang X ,Ren H J, Xie B, et al., MoX_2 (X = O, S) Hierarchical Nanosheets Confined in Carbon Frameworks for Enhanced Lithium-Ion Storage. ACS Appl. Nano Mater. 2021, 4(5): 4615 – 4622.

[22] Wang Z, Chen J S, et al., ChemInform abstract: one-pot synthesis of uniform carbon-coated MoO_2, nanospheres for high-rate reversible lithium storage. Chem Commun 2010, 41(50): 6906 – 6908.

[23] Borghols W J H,Wagemaker M, et al., Size Effects in the $Li_{4+x}Ti_5O_{12}$ Spinel. J Am Chem Soc 2009, 131: 17786-17792.